Original Article
Cite This: Colloid & Nanoscience Journal 1 (2023) 154-162.
CNJ.araku.ac.ir

Synthesis and characterization of the ZnO-supported on clinoptilolite as a nanophotocatalyst and malachite green dye photodegradation

Saeid Najafi*[1], Javad Saien[2]

Received: 2023-09-09
Revised: 2023-09-19
Accepted: 2023-09-20
DOI: **10.61186/CNJ.1.3.154**

[1]Dipartimento di Chimica "Ugo Schiff" - Università degli Studi di Firenze, Via della Lastruccia, 3, 50019 Sesto Fiorentino FI, Italy
[2]Faculty of Chemistry, Bu-Ali Sina University, Hamedan, 651783868, Iran

Abstract

In this investigation, a novel type of zinc oxide supported on clinoptilolite zeolite ZnO /Clinoptilolite (ZnO/CP) nanophotocatalyst was prepared based on the solid-state dispersion (SSD) method. The prepared nanophotocatalyst was characterized with XRD, BET and SEM techniques. As an application, the photocatalytic degradation of malachite green dye (MG) in water under UV irradiation was studied. The results show that the ZnO/CP is an active nanophotocatalyst and the maximum effect of MG photodegradation was observed at 10 wt.% ZnO, 90 wt% Clinoptilolite. Based on the obtained results, a first-order reaction with k = 0.0075 min^{-1} was concluded. The effects of some parameters such as pH, amount of photocatalyst, and temperature were also examined. Finally, a mechanism was introduced for MG.

Keywords: Photodegradation, Nanophotocatalysts, ZnO Nanoparticles, Malachite green, Clinoptilolite

1. Introduction

From the viewpoint of green chemistry, the photocatalytic decomposition of organic compounds in wastewater has attracted a great deal of attention [1,2].

photocatalysis based on the nanomaterials as an alternative or complementary technology for water purification systems were investigated as smart due to the excellent surface area and morphological properties material since these reactions are normally regulated by a mechanism of free radicals such as reacrtive oxygen species($^{\bullet}OH$, $O_2^{\bullet -}$, $H_2O^{\bullet}$). ZnO nanoparticles are one of the most effective nanophotocatalysts because it is biologically and chemically inert and photostable with near-UV band gap energy. ZnO can be used as a fine powder or crystals dispersed in water wastewater treatment applications. However, the need to filter ZnO after reaction makes such a process troublesome and costs. Thus, in order to solve this problem, many researchers have examined some methods for fixing ZnO on supporting materials including glass beads [3], fiberglass [4], silica [5], and zeolite [6]. When using zeolite as ZnO support, care should be taken that ZnO does not lose its photo activity and the adsorption properties of zeolite are not affected. Mattews [3] showed the photoefficiency of ZnO is suppressed when Ti is in interaction with the zeolite.

A variety of methods were reported for the fabrication of the nanophotocatalyst and nanocomposite. A microemulsion system as a soft template [6-8] is the most effective route for controlling the size and monodispersity of the nanoparticles in matrix [9-13] to create charge carriers without recombination and photocatalytic performance limitations [13-17]. Mirhoseini and Salabat prepared a novel type of photocatalyst as visible light active nanocomposite in ionic liquid-based microemulsion for the removal of water pollutants, and also as an antibacterial agent [18-25].

In this work ZnO was supported on a Clinoptilolite (CP) zeolite without losing photo efficiency with the synergistic effect of adsorption and a photocatalysis system was prepared by solid-state dispersion (SSD) method and used for photodegradation of the Malachite Green dye (MG) under UV illumination. A variety of operating parameters were also investigated in detail and a mechanism was introduced.

2. Experimental

2.1. Materials

Clinoptilolite zeolite powder (from Center of Geological Survey of Iran) with the average particle size of 105 micrometer and the chemical composition of SiO_2 64.43%, Al_2O_3 12.80%, Fe_2O_3 1.31%, TiO_2 0.31%, CaO 2.58%, MgO 1.28%, Na_2O 1.23%, K_2O 2.64%, P_2O_5 0.21%, PbO 13.19% was used as photocatalyst matrix. Zinc nitrate ($Zn(NO_3)_2$ as a metal source, HCl and NaOH for pH adjustment, malachite green dye and sodium dodecyl sulfate as surfactant were purchased from the Merck company. The molecular structure of MG is shown in Fig.1.

Corresponding Authors: Saeid Najafi
saeid.najafi@stud.unifi.it

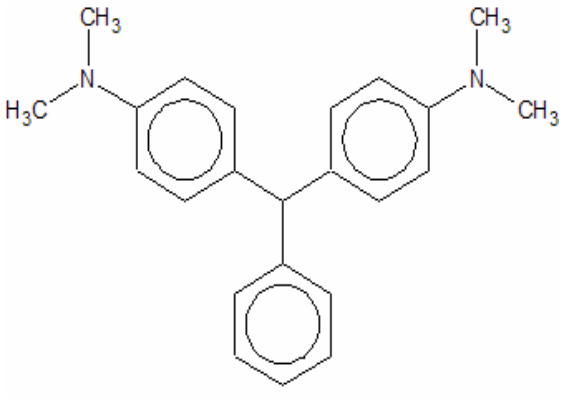

Schem. 1. The molecular structure of MG dye

2.2. Preparation of ZnO - supported CP nanophotocatalyst

The solid-state dispersion (SSD) method was used for preparing the Zeolite-based photocatalyst. In this method, precipitation method in liquid phase was used to prepare ZnO stabilized on CP zeolite. In this method, first a saturated solution of zinc nitrate solution was prepared, and then Clinoptilolite zeolite was added to the zinc precursor solution by weight of 1:1 zinc nitrate. Then two drops of the surfactant (sodium dodecyl sulfate) was added and the system was stirred for 2 hours and titrated with 5M NaOH solution. After adding NaOH solution, the mixture was poured into the test tube and centrifuged at a speed of 5000 RPM for 10 minutes, and the resulting precipitate ($Zn(OH)_2$) was dissolved with the NaOH solution. The resulting solution was filtered and washed with ethanol. and then sonicated for 6 min. The ($Zn(OH)_2$)/CP was placed in the oven at 110 °C for 2 hours and calcined at 450 °C for 5 hours to form zinc oxide nanoparticles on the surface of the CP.

2.3. Characterization

The morphology of the nanophotocatalyst was observed using scanning electron microscopy (SEM). Prior to being loaded into SEM, the sample was dispersed in ethanol, sonicated, and dropped onto a wholly carbon-coated copper grid and was applied by Philips XL30 instrument. X-ray diffraction (XRD) measurements were carried out on nanocatalyst using a Philips PW 1800 diffractometer with a Cu Ka radiation and Ni filter. Brunauer–Emmett–Teller (BET) as the basis for an important analysis technique for the measurement of the specific surface area of materials using (Micromeritic-2100E) was used to explain the physical adsorption of gas molecules on a solid surface of the prepared ZnO/CP nanophotocatalyst.

2.4. Photocatalytic study

The batch reactor was made of pyrex glass with a double wall and a volume of 4 liters, and a mirror was designed to increase the reactor's opening (Fig. 1). There is no air in the space between the two walls. The homogenization of the contents inside the reactor is done by aerating the solution with an air pump. Six UV lamps with a power of 8 W are placed directly in the solution after proper insulation.

The lamps used in this process were manufactured by Hitachi Company, with a diameter of 1 cm and a length of 20 cm. These lamps are low-pressure mercury lamps that produce C-type ultraviolet rays. Aeration was done by an air pump manufactured by Damandeh, Iran, model (XP-3600) with an operating voltage of 220 V and a power of 8 W with a flow rate of 1 L.min-1. The bubbles created by the pump were transferred to the lower part of the reactor with a hose and exited from the top. A thermometer made by HAnyoung Company in Japan was used to regulate the reactor temperature during the experiment with Multi-input, Rele output, 4 digits; it has a temperature range of 0-200 ºC and a voltage of v220. The thermocouple which is connected to the thermo bat was type: K with a diameter of 6mm and a length of 15cm and made of stainless steel. In order to carry out the photocatalytic degradation of dye examination, all samples including the pure ZnO nanoparticles, ZnO supported on the CP, were added to the dye solutions (in terms of ppm) separately and then the pH of the solution was adjusted by adding dilute NaOH and H_2SO_4 (0.5 M). For pH adjustment, a py-p12 electrode and Sartorius PT-10P pH meter were used. The solution is placed in the dark for 30 minutes to achieve equilibrium conditions. The resulting solution was introduced into the batch reactor and exposed to UV-C radiation. The dye solution was sampled in an interval of 10 min and was measured using a UV-VIS spectrophotometer (Perkin-Elmar model (lambda was 25. during the measurement). Then sampled solution was added to the reactor to continue the photodegradation study. The concentration of the samples was determined using a spectrophotometer (UV/VIS Spectrophotometer, Perkin-Elmer lambda 25) at λ_{ma}=617.38 nm. The degree of photodegradation (X) as a function of time is given by:

$$X = \frac{[MG]_0 - [MG]}{[MG]_0} \quad (1)$$

Where $[MG]_0$ and $[MG]$ are the concentration of dye at t = 0 and t, respectively. Two tests was done as a comparative study at the same condition with only UV irradition without catalyst and in presnt ot CP matrix. The photodecolorization rate constant (k) was calculated by plotting ln C_0/C versus times based on the first order reaction according to eq. (2).

$$\ln C_0/C = kt \quad (2)$$

In this equation, k represents the rate constant (min^{-1}).

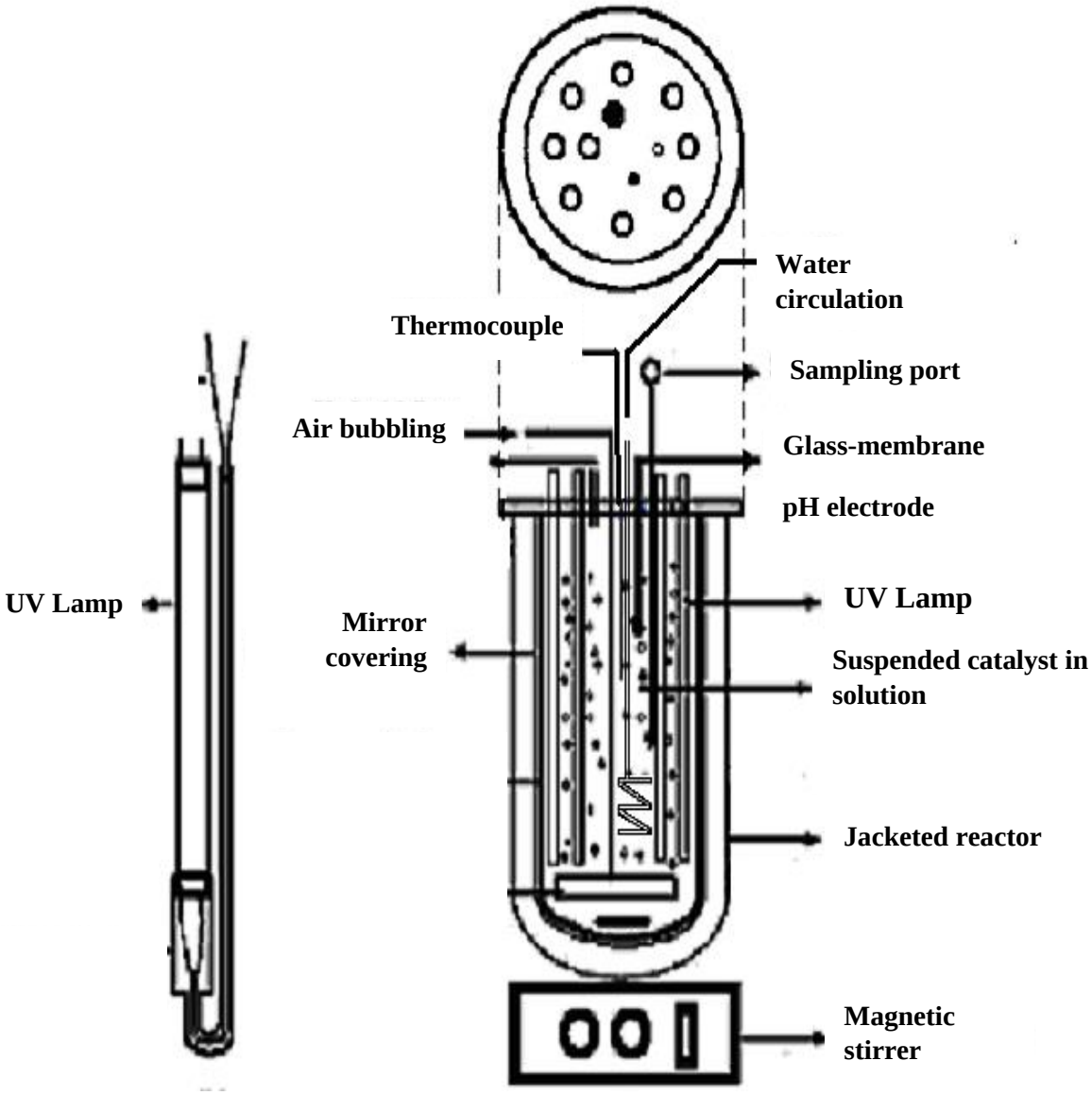

Fig. 1. The batch reactors for photodegradation of MG dye under UV irradiation.

3. Results and discussion

3.1. XRD analysis

The effective samples in the photocatalytic process, the same ratio obtained in the previous experiments, were used to prepare XRD patterns. The XRD patterns are shown in Fig. 2. Since there is ZnO in the primary zeolite structure and since no change in the appearance of the mentioned peaks was observed, it can be concluded that there is no remarkable change in the crystal structure of ZnO during the fixation of ZnO on the surface of the zeolite as a matrix. Therefore, the increase in the intensity of the mentioned peaks in XRD also indicates the increase in the amount of ZnO in the zeolite structure.

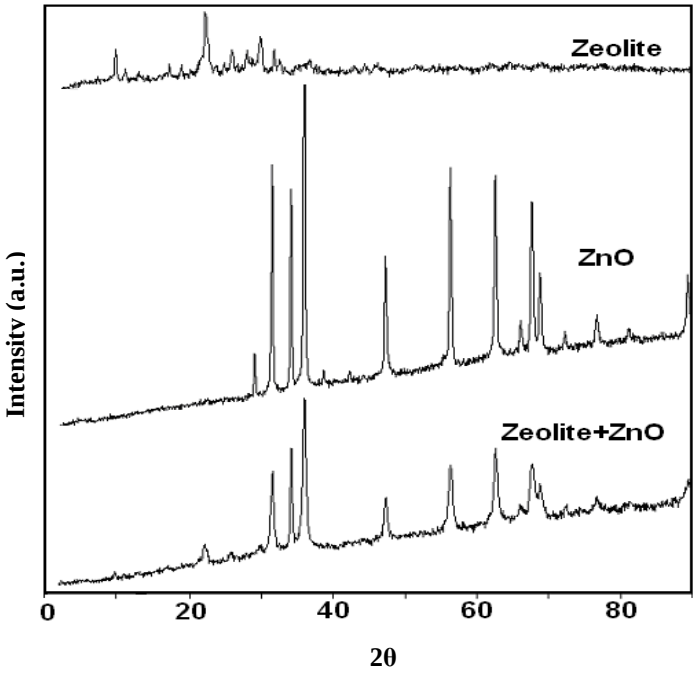

Fig. 2. XRD patterns of pure CP zeolite, ZnO nanoparticles and ZnO/CP zeolite nanophotocatalyst calcined at 450 °C.

3.2. SEM images and BET study

The SEM images obtained from the nanocatalyst are shown in Fig. 3. As can be seen from images, it has been determined that the size of ZnO particles is larger than that to penetrate into the pores and be fixed there, because according to the SEM images, the dimensions of zinc oxide particles are larger than the dimensions of the holes and pores in Clinoptilolite zeolite (It is one about nanometer) [9]. SEM images also revealed that the surface morphology of zeolites changed after ZnO stabilization. In the SEM images of nanocatalyst, it is well shown how the ZnO nanoparticles are placed and fixed on the crystal parts of the Clinoptilolite zeolite.

BET measurements of ZnO/Clinoptilolite nanophotocatalyst also showed that the surface of zeolite decreased from 1480 m^2g^{-1} to 418 m^2g^{-1}. These results confirm the change in the catalyst's surface morphology, the covering of the zeolite surface, and the opening of its holes with the ZnO catalyst.

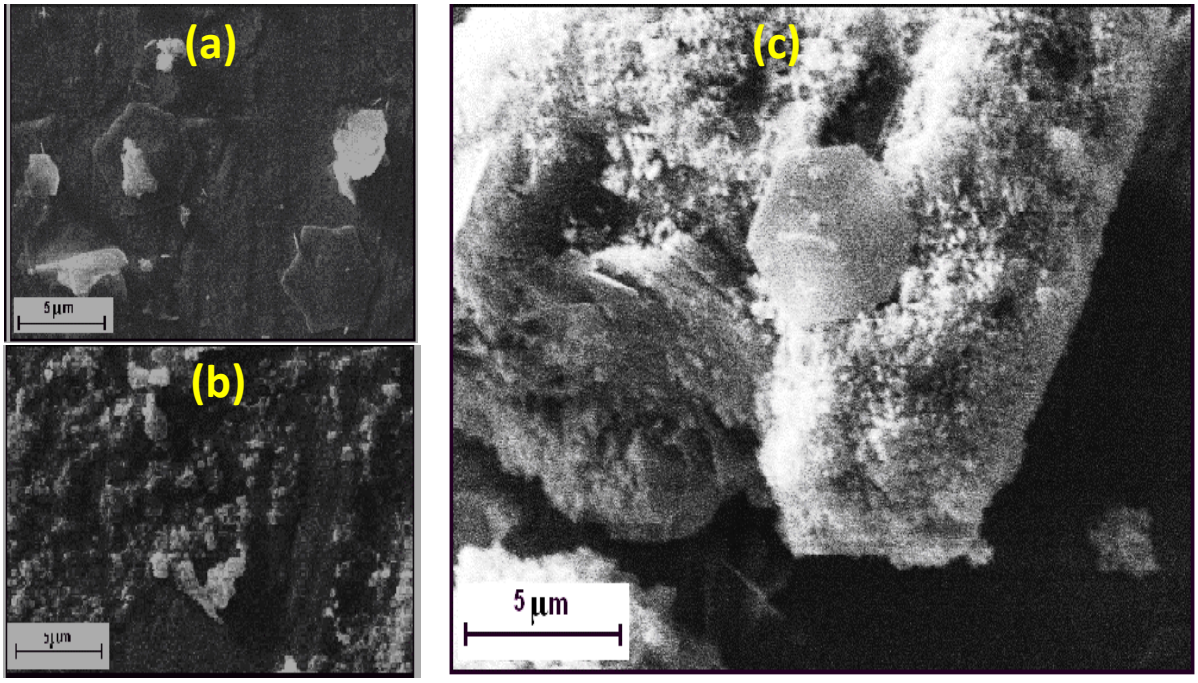

Fig. 3. The SEM images of (a) ZnO nanoparticles, (b) CP zeolite, and (c) ZnO/CP nanophotocatalyst.

3.3. Photocatalytic investigation

The absorbances of MG solutions during the photocatalytic process at initial and after 2 h irradiation time versus λ are shown in the Fig 4. The spectrum of MG in the visible region exhibits a main band with a maximum at 617.38 nm. The decrease of absorption peaks of MG at λ_{max}=617.38 nm in this Fig. indicates a rapid degradation of the dye.

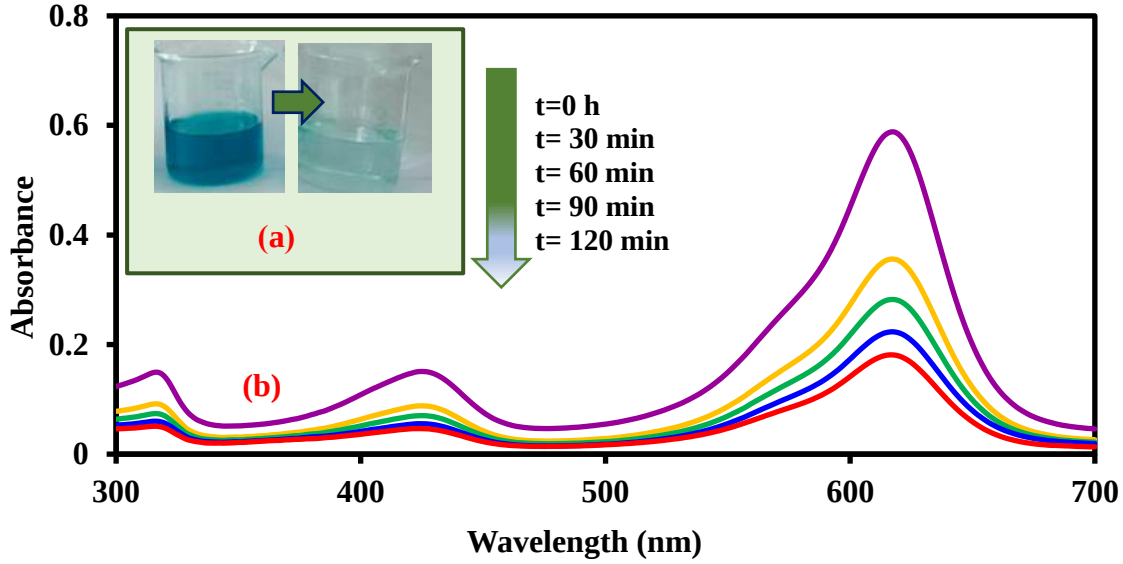

Fig. 4. (a) Photographic images MG dye after degradation at different time intervals, (b) UV-VIS spectra of MG paint (under the conditions: 298K and initial MG dye concentration equal to 5 ppm and pH = 8.5 and photocatalyst amount equal to 0.8 mg per four liters of dye solution) at times between t=0 and t=120 min, in the presence of the catalyst fixed on CP zeolite.

The effect of the nanophotocatalyst irradiation on the photodegradation of MG is shown in Fig. 5-a, This Fig. shows that in the presence of nanocatalyst (ZnO/CP) and UV irradiation, 70% of the MG dye was decomposed within 120 min of irradiation, while 33% was decomposed for ZnO (without CP matrix).These experiments prove that both UV light illuminiation and ZnO/CP nanophotocatalyst are required for efficient MG degradation. Fig. 5-b, presents the plot of reciprocal of pseudo-first order rate constant against initial concentration of MG=5 ppm, concentration of photocatalyst = 40 ppm, T = 298 K, pH=9.5, and result shows the rate constant is 0.0075 min^{-1}.

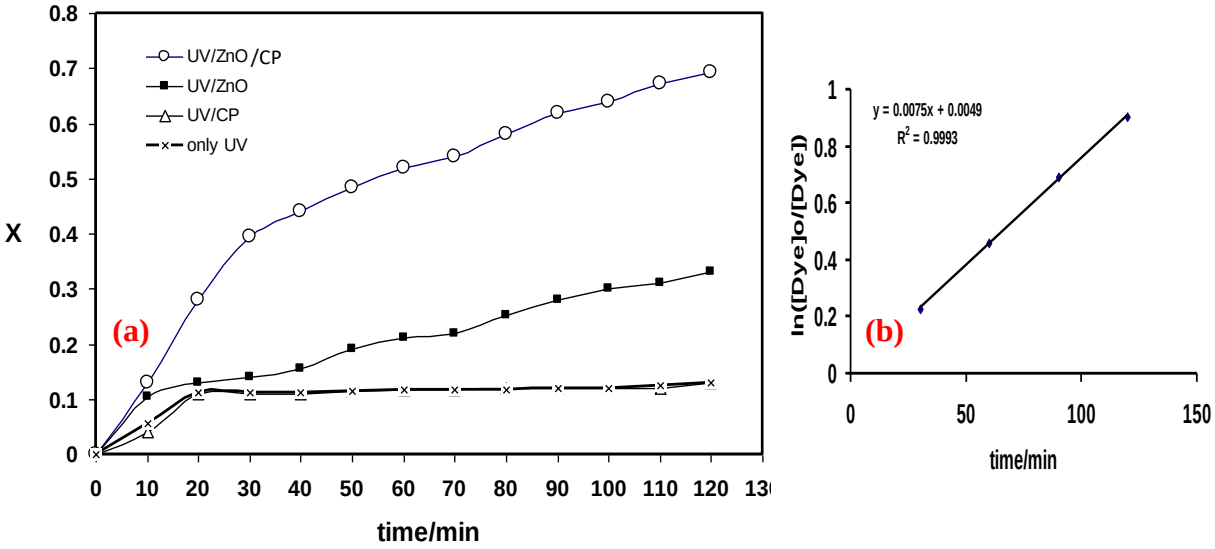

Fig. 5. (a) Photocatalytic activity of all samples for degradation of MG dye under UV irradaiation, (b) Plot of reciprocal of pseudo-first order rate constant against initial concentration of MG=5 ppm, concentration of photocatalyst = 40 ppm, T = 298 K, pH=9.5.

3.4. The effect of catalyst concentration

At this study, the effect of different amounts of catalyst between 0.4 and 1.2 mg/L of dye solution was tested. The results in Fig. 6 show that by increasing the catalyst concentration up to 200 ppm, the reaction speed increased and by increasing the catalyst concentration above this value, the reaction speed decreased. The reason for the reduction of photocatalytic activity in concentrations higher than 200ppm is that with the increase in the amount of photocatalyst, the phenomenon of light scattering occurred due to the collision of light rays with the catalyst particles dispersed in the solution, and a number of light photons lost their energy that is caused the recombination of charge carriers as a main limitation in photocatalysis systems.

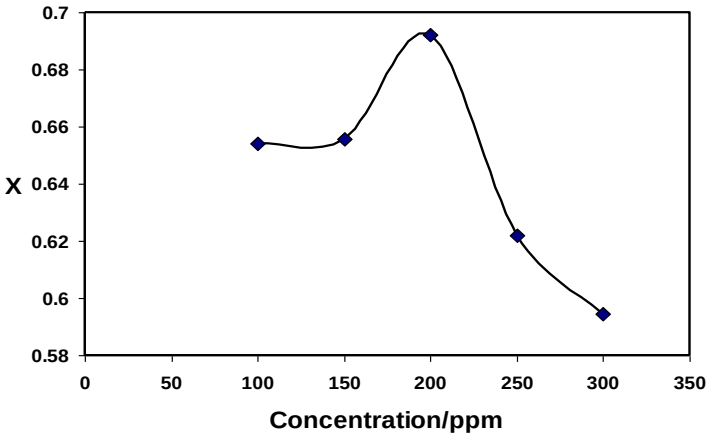

Fig. 6. The Effect of nanophotocatalyst concentration for degradation of MG dye under UV irradiation, T = 298 K, $X = \frac{[MG]_0 - [MG]}{[MG]_0}$

3.5. The effect of pH

pH is one of the main factors influencing the rate of degradation of some organic compounds in the photocatalytic process [15,16]. It is also an important operational variable in wastewater treatment. Fig.5 shows the photodegradation of MG at different pH from 5.5 to 9.5, which shows that the best results were obtained in pH =9.5 of solution. The suggested mechanism can be described as follow:

$$e^-_{CB} + O_{2(ads)} \longrightarrow {}^{\bullet}O^-_{2(ads)} \quad (1)$$

$${}^{'}O^-_{2(ads)} + H^+ \longrightarrow HO^{\bullet}_2 \quad (2)$$

$$2HO^{\bullet}_2 \longrightarrow O_2 + H_2O_2 \quad (3)$$

$$H_2O_2 + {}^{\bullet}O^-_{2(ads)} \longrightarrow {}^{\cdot}OH + OH^- + O_2 \quad (4)$$

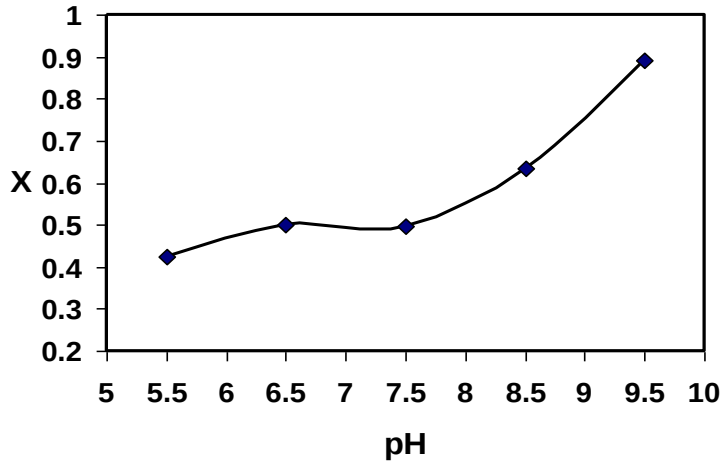

Fig. 7: The effect of pH on photodegradation efficiency of MG, [MG]o = 5 ppm, concentration of photocatalyst = 20 ppm, T = 298 K, $X = \frac{[MG]_0 - [MG]}{[MG]_0}$

3.6. The effect of temperature on MG photodegradation

The results shown in Fig. 8 show the positive effect of temperature on color decomposition. An increase in temperature from 20°C to 35°C indicates that the percentage of color change increases with increasing temperature. It should be mentioned that the reason why the temperature higher than 35 degrees Celsius was not chosen was that at higher temperatures, the possibility of evaporation of the solution increased and it caused the color concentration to change due to the evaporation of the solvent. Since the electron transfer from the conduction band to higher levels in semiconductors has been done at a higher speed with the increase in temperature, therefore the activation process and in other words the number of active sites of the catalyst has increased and the result of this is the increase in the rate of photodecomposition. To determine the E_a *the* graph of $-ln\,k$ as 1/T was drawn and based on the Arrhenius equation ($-\ln k = \frac{E_a}{RT} - \ln A$), the value of the Arrhenius constant (A) has been obtained from the slope of the above-mentioned drawn line and using the width from the origin of the mentioned line. The value of the 27.515 $(kJ/mol.K)$ and 517.7 for A was calculated.

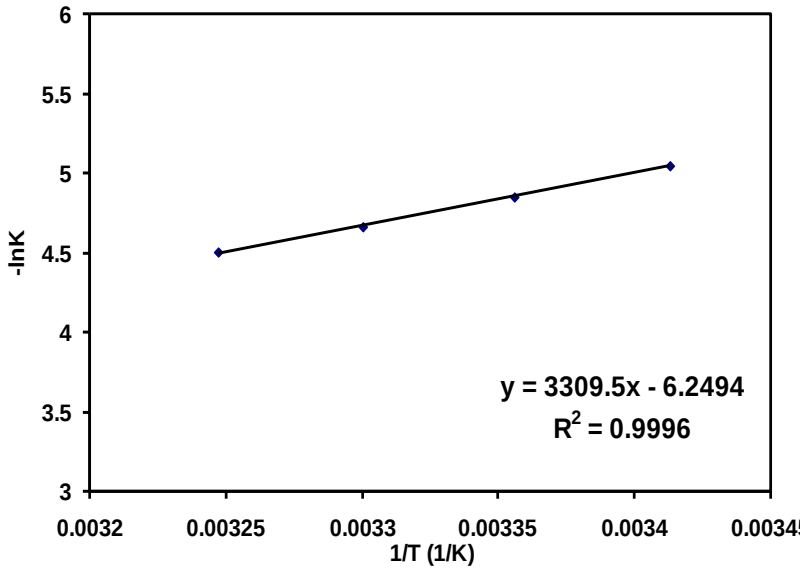

Fig. 8. The effect of temperature on the photocatalytic decomposition of MG dye (in the conditions where the initial dye concentration was 5 ppm, the photocatalyst concentration was 20 mg/lit and pH = 9.5)

3.7. Proposed mechanism

The electronic structure of ZnO semiconductors includes a valance band and an empty conduction band. When the energy of the photon (hU) is equal to or greater than the electron transfer energy between these two bands, which is called the energy gap (E_g) in the semiconductor, an electron is excited from the valance band (VB) to the conduction band (CB) and leaves a hole in the VB. The VB potential is positive enough to generate hydroxyl radicals and the CB potential is negative enough to reduce molecular oxygen. The hydroxyl radical is a strong oxidizing agent and adsorbs organic contaminants on or near the ZnO surface. This phenomenon causes photo-oxidation of color based on the following reactions [6-8,26].

$$ZnO + h\nu \rightarrow ZnO\,(e^-_{CB} + h^+_{VB}) \quad (5)$$

$$h^+_{VB} + H_2O_{(ads)} \rightarrow H^+ + {}^{\bullet}OH_{(ads)} \quad (6)$$

$$h^+_{VB} + OH^-_{(ads)} \rightarrow {}^{\bullet}OH_{(ads)} \quad (7)$$

$$e^-_{CB} + O_{2(ads)} \rightarrow {}^{\bullet}O^-_{2(ads)} \quad (8)$$

$${}^{\bullet}O^-_{2(ads)} + \text{dye} \rightarrow \text{dye-OO}^{\bullet} \quad (9)$$

$$h^+_{VB} + \text{dye} \rightarrow \text{dye}^{\bullet+} \rightarrow \text{oxidation of the dye} \quad (10)$$

$${}^{\bullet}O^-_{2(ads)} + HO^{\bullet}_{2(ads)} + H^+ \rightarrow H_2O_{2(ads)} + O_{2(ads)} \quad (11)$$

$${}^{\bullet}OH_{(ads)} + \text{dye} \rightarrow \text{degradation of the dye} \quad (12)$$

4. Conclusion

In this study, the SSD method as an effective method was used for preparation of the ZnO/ clinoptilolite. The prepared nanophotocatalyst was characterized with XRD, BET and SEM analysis. The photocatalyst containing 10% ZnO and 90% clinoptilolite has the maximum photodegradation efficiency for MG removal. The photodegradation conversion of MG decreases with an increase in the initial concentration of MG. pH is one of the main affecting factors and the optimum pH is about 9.5. Kinetics of photocatalytic degradation of MG was studied and a pseudo-first order with k=0.0075 min^{-1} obtained.

Conflicts of Interest

The author declares no conflict of interest.

Author information

*Corresponding Author: Saeid Najafi
saeid.najafi@stud.unifi.it

ORCID
Javad Saien: 0000-0001-5731-0227

References

[1] M.B. Tahir, T. Nawaz, G. Nabi, M. Sagir, M.I. Khan, N. Malik, Role of nanophotocatalysts for the treatment of hazardous organic and inorganic pollutants in wastewater. International Journal of Environmental Analytical Chemistry, 102(2) (2022) 491–515. https://doi.org/10.1080/03067319.2020.1723570
[2] M.A. Fox, K.E. Doan, M.T. Dulay, The effect of the “Inert” support on relative photocatalytic activity in the oxidative decomposition of alcohols on irradiated titanium dioxide composites. Research on Chemical Intermediates, 20(7) (1994) 711–721. https://doi.org/10.1163/156856794x00504.
[3] R.W. Matthews, S.R. McEvoy, Destruction of phenol in water with sun, sand, and photocatalysis, Solar Energy, 49, 1992, 507-513. https://doi.org/10.1016/0038-092X(92)90159-8.
[4] C.S. Turchi, D.F Ollis, Comment. Photocatalytic reactor design: an example of mass-transfer limitations with an immobilized catalyst, Phys. Chem., 92, 1988, 6852-6853. https://doi.org/10.1021/j100334a070
[5] G. P. Lepore, L. Persaud, C. H. Langford, Supporting titanium dioxide photocatalysts on silica gel and hydrophobically modified silica gel, J. Photoche. Photobiol. A: Chem., 98, (1996) 103-111. https://doi.org/10.1016/1010-6030(95)04242-3.
[6] M.N. Chrétien, Supramolecular photochemistry in zeolites: From catalysts to sunscreens, Pure App.Chem., 79, 2007, 1-20. https://doi.org/10.1351/pac200779010001
[7] A. Salabat, F. Mirhoseini, Polymer-based nanocomposites fabricated by microemulsion method, Polym. Compos. 43 (2022) 1282–94. https://doi.org/10.1002/pc.26504
[8] A. Salabat, F. Mirhoseini, M. Mahdieh, H. Saydi, A novel nanotube-shaped polypyrrole-Pd composite prepared using reverse microemulsion polymerization and its evaluation as an antibacterial agent, New J. Chem. 39 (5) (2015) 4109–4114. https://doi.org/10.1039/c5nj00175g
[9] A. Salabat, F. Mirhoseini, M. Arjomandzadegan, E. Jiryaei, A novel methodology for fabrication of Ag-polypyrrole core-shell nanosphere using microemulsion system and evaluation of its antibacterial application, New J. Chem. 41 (21) (2017) 12892–12900. https://doi.org/10.1039/c7nj00678k
[10] A. Salabat, F. Mirhoseini, R. Valirasti, Engineering poly(methyl methacrylate)/Fe_2O_3 hollow nanospheres composite prepared in microemulsion system as a recyclable adsorbent for removal of benzothiophene, Ind. Eng. Chem. Research 58 (2019) 17850-1785. https://doi.org/10.1021/acs.iecr.9b04322
[11] A. Salabat, F. Mirhoseini, K. Abdoli, A microemulsion route to fabrication of mono and bimetallic Cu/Zn/γ-Al_2O_3 nanocatalysts for hydrogenation reaction. Scientia Iranica, 25(2018) 1364-1370. https://doi.org/10.24200/sci.2018.5023.1048
[12] B.S. Mirhoseini, A. Salabat, A novel surfactant-free microemulsion system for the synthesis of poly(methyl methacrylate)/Ag nanocomposite, J. Mol. Liq. 342 (2021) 117555. https://doi.org/10.1016/j.molliq.2021.117555
[13] A. Salabat, F. Mirhoseini, Z. Masoumi, M. Mahdie, Preparation and characterization of polystyrene-silver nanocomposite using microemulsion method and its antibacterial activity, JNS 4 (2014) 377-382.
[14] F. Alimohamadi, A. Salabat, Effect of surfactant type on the particle dispersion in Ag/polystyrene nanocomposite prepared by microemulsion method, Colloid Nanosci. J. 1 (2023) 112-118. https://doi.org/10.52547/CNJ.1.2.112
[15] A. Salabat, F. Mirhoseini, A novel and simple microemulsion method for synthesis of biocompatible functionalized gold nanoparticles, J. Mol. Liq. 268 (2018) 849–853. https://doi.org/10.1016/j.molliq.2018.07.112

[16] F. Kamali, K. Faghihi, F. Mirhoseini, High antibacterial activity of new eco-friendly and biocompatible polyurethane nanocomposites based on Fe_3O_4/Ag and starch moieties. Polym. Eng. Sci., 62(5) (2022) 1444-1462.https://doi.org/10.1002/pen.25934
[17] A. Salabat, F. Mirhoseini, F.H. Nouri, Microemulsion strategy for preparation of TiO_2–Ag/poly(methyl methacrylate) nanocomposite and its photodegradation application. J. Iranian Chem. Soc. 20 (2022) 599–608. https://doi.org/10.1007/s13738-022-02693-7.
[18] F. Mirhoseini, Alireza Salabat, Ionic liquid based microemulsion method for fabrication of poly(methyl methacrylate)–TiO_2 nanocomposite as highly efficient visible light photocatalyst, RSC Adv. 5 (2015) 12536–12545. https://doi.org/10.1039/c4ra14612c
[19] F. Mirhoseini, Alireza Salabat, Iinvestigation of operational parameters on the photocatalytic activity of a new type of poly(methyl methacrylate)/ionic liquid-tio_2 nanocomposite, Iranian J. Chem. Chem. Eng., 38 (2019) 101-114. https://doi.org/10.30492/IJCCE.2019.37613
[20] F. Mirhoseini, Alireza Salabat, Photocatalytic filter, United States patent 10828629.
[21] A. Salabat, F. Mirhoseini, Applications of a new type of poly(methyl methacrylate)/TiO_2 nanocomposite as an antibacterial agent and a reducing photocatalyst. Photochem. Photobiol. Sci., 14(9) (2015) 1637–1643. https://doi.org/10.1039/c5pp00065c
[22] F. Mirhoseini, Alireza Salabat, Removal of methyl tert -butyl ether as a water pollutant by photodegradation over a new type of poly(methyl methacrylate)/TiO_2 nanocomposite. Polymer Composites, *39*(4) (2018) 1248–1254. https://doi.org/10.1002/pc.24059
[23] F. Mirhoseini, A. Salabat, Antibactrial activity based poly(methyl methacrylate) supported TiO_2 photocatalyst film nanocomposite, Tech. J. Eng. Appl. Sci. 5 (2015)115-118.
[24] A. Salabat, F. Mirhoseini, Photo-induced hydrophilicity study of poly(methyl methacrylate)/TiO_2 nanocomposite prepared in ionic liquid based microemulsion system. Current Appl. Polym. Sci., 2(2), (2018) 112–120. https://doi.org/10.2174/2452271602666180803141554
[25] F. Mirhoseini, A. Salabat, Polymer nanocomposite based composition and method for controlling water hardness, United States patent 11136247.
[26] R. Amini, G. Nabiyouni, S. Jarollahi, Removal of azo dyes pollutants: photocatalyst and magnetic investigation of iron oxide-zinc sulfide nanocomposites, JNS 11 (1) (2021) 95-104.